

Malware Classification with GMM-HMM Models

Jing Zhao*

Samanvitha Basole[†]

Mark Stamp[‡]

March 5, 2021

Abstract

Discrete hidden Markov models (HMM) are often applied to malware detection and classification problems. However, the continuous analog of discrete HMMs, that is, Gaussian mixture model-HMMs (GMM-HMM), are rarely considered in the field of cybersecurity. In this paper, we use GMM-HMMs for malware classification and we compare our results to those obtained using discrete HMMs. As features, we consider opcode sequences and entropy-based sequences. For our opcode features, GMM-HMMs produce results that are comparable to those obtained using discrete HMMs, whereas for our entropy-based features, GMM-HMMs generally improve significantly on the classification results that we have achieved with discrete HMMs.

1 Introduction

Due to COVID-19, businesses and schools have moved their work online and some consider the possibility of going online permanently. This trend makes cybersecurity more important than ever before.

Malicious software, or malware, is designed to steal private information, delete sensitive data without consent, or otherwise disrupt computer systems. The study of malware has been active for decades (Milosevic, 2013). Malware detection and classification are fundamental research topics in malware. Traditionally, signature detection has been the most prevalent method for detecting malware, but recently, machine learning techniques have proven their worth, especially for dealing with advanced types of malware. Many machine learning approaches have been applied to the malware problem, including hidden Markov models (HMM) (Stamp, 2018), k -nearest neighbors (KNN) (Ben Abdel Ouahab et al., 2020), support vector machines (SVM) (Kruczkowski and Szykiewicz, 2014), and a wide variety of neural networking and deep learning techniques (Kalash et al., 2018).

Each machine learning technique has its own advantages and disadvantages. It is not the case that one technique is best for all circumstances, since there are many different types of malware and many different features that can be considered. Thus, it is useful to explore different techniques and algorithms in an effort to extend our knowledge base for effectively dealing with malware. In this paper, we focus on Gaussian mixture model-hidden Markov models (GMM-HMMs), which can be viewed as the continuous analog of the ever-popular discrete HMM.

Discrete HMMs are well known for their ability to learn important statistical properties from a sequence of observations. For a sequence of discrete observations, such as the letters that comprise a selection of English text, we can train a discrete HMM to determine the parameters of the (discrete) probability distributions that underlie the training data. However, some observation sequences are inherently continuous, such as signals extracted from speech. In such cases, a discrete HMM is not the ideal tool. While we can discretize a continuous signal, there will be some loss of information. As an alternative to discretization, we can attempt to model the continuous probability density functions that underlie continuous training data.

Gaussian mixture models (GMM) are probability density functions that are represented by weighted sums of Gaussian distributions (Reynolds, 2015). By varying the number of Gaussian components

*jing.zhao@sjsu.edu

[†]s97basole@gmail.com

[‡]mark.stamp@sjsu.edu

and the weight assigned to each, GMMs can effectively model a wide variety of continuous probability distributions. It is possible to train HMMs to learn the parameters of GMMs, and the resulting GMM-HMM models are frequently used in speech recognition (Rabiner, 1989; Bansal et al., 2008), among many other applications.

In the field of cybersecurity, GMMs have been used, for example, as a clustering method for malware classification (Interrante-Grant and Kaeli, 2018). However, to the best of our knowledge, GMM-HMMs are not frequently considered in the context of malware detection or classification. In this paper, we apply GMM-HMMs to the malware classification problem, and we compare our results to discrete HMMs. Our results indicate that GMM-HMMs applied to continuous data can yield strong results in the malware domain.

The remainder of this paper is organized as follows. In Chapter 2, we discuss relevant related work. Chapter 3 provides background on the various models considered, namely, GMMs, HMMs, and GMM-HMMs, with the emphasis on the latter. Malware classification experiments and results based on discrete features are discussed in Chapter 4. Since GMM-HMMs are more suitable for continuous observations, in Chapter 4 we also present a set of malware classification experiments based on continuous entropy features. We conclude the paper and provide possible directions for future work in Chapter 5.

2 Related Work

A Gaussian mixture model (GMM) is a probability density model (McLachlan and Peel, 2004) consisting of a weighted sum of multiple Gaussian distributions. The advantage of a Gaussian mixture is that it can accurately model a variety of probability distributions (Gao et al., 2020). That is, a GMM enables us to model a much more general distribution, as compared to a single Gaussian. Although the underlying distribution may not be similar to a Gaussian, the combination of several Gaussians yields a robust model (Alfakih et al., 2020). However, the more Gaussians that comprise a model, the costly the calculation involving the model.

One example of the use of GMMs is distribution estimation of wave elevation in the field of oceanography (Gao et al., 2020). GMMs have also been used in the fields of anomaly detection (Chen and Wu, 2019), and signal mapping (Raitoharju et al., 2020). As another example, in (Qiao et al., 2019), a GMM is used as a classification method to segment brain lesions. In addition to distribution estimation, GMMs form the basis for a clustering method in (Gallop, 2006).

As the name suggests, a discrete hidden Markov model (HMM) includes a “hidden” Markov process and a series of observations that are probabilistically related to the hidden states. An HMM can be trained based on an observation sequence, and the resulting model can be used to score other observation sequences. HMMs have found widespread use in signal processing, and HMMs are particularly popular in the area of speech recognition (Guoning Hu and DeLiang Wang, 2004). Due to their robustness and the efficiency, HMMs are also widely used in medical areas, such as sepsis detection (Stanculescu et al., 2014) and human brain studies based on functional magnetic resonance imaging (Dang et al., 2017). Motion recognition is another area where HMMs play a vital role; specific examples include recognizing dancing moves (Laraba and Tilmanne, 2016) and 3D gestures (Truong and Zaharia, 2017).

Gaussian mixture model-HMMs (GMM-HMM) are also widely used in classification problems. Given the flexibility of GMMs, GMM-HMMs are popular for dealing with complex patterns underlying sequences of observations. For example, Yao et al. (Yao et al., 2020) use GMM-HMMs to classify network traffic from different protocols. GMM-HMMs have also been used in motion detection—for complex poses, GMM-HMMs outperform discrete HMMs (Zhang et al., 2020).

3 Background

In this section, we first introduce the learning techniques used in this paper—specifically, we discuss Gaussian mixture models, HMMs, and GMM-HMMs. We then discuss GMM-HMMs in somewhat more detail, including various training and parameter selection issues, and we provide an illustrative example of GMM-HMM training.

3.1 Gaussian Mixture Models

As mentioned above, a GMM is a probabilistic model that combines multiple Gaussian distributions. Mathematically, the probability density function of a GMM is a weighted sum of M Gaussian probability density functions. The formulation of a GMM can be written as (Fraley and Raftery, 2002)

$$P(x|\lambda) = \sum_{x=i}^M \omega_i g(x|\mu_i, \Sigma_i),$$

where x is a D -dimensional vector and ω_i is the weight assigned to the i^{th} Gaussian component, with the mixture weights summing to one. Here, μ_i and Σ_i are the mean and the covariance matrix of the i^{th} component of the GMM, respectively. Each component of a GMM is a multivariate Gaussian distribution of the form

$$g(x|\mu_i, \Sigma_i) = \frac{1}{(2\pi)^{\frac{D}{2}} |\Sigma_i|^{\frac{1}{2}}} e^{-\frac{1}{2}(x-\mu_i)'\Sigma_i^{-1}(x-\mu_i)}.$$

3.2 Discrete HMM

In this paper, we use the notation in Table 1 to describe a discrete HMM. This notation is essentially the same as that given in (Stamp, 2018). An HMM, which we denote as λ , is defined by the matrices A , B , and π , and hence we have $\lambda = (A, B, \pi)$.

Table 1: Discrete HMM notation

Notation	Explanation
T	Length of the observation sequence
O	Observation sequence, O_0, O_1, \dots, O_{T-1}
N	Number of states in the model
K	Number of distinct observation symbols
Q	Distinct states of the Markov process, q_0, q_1, \dots, q_{N-1}
V	Observable symbols, assumed to be $0, 1, \dots, K-1$
π	Initial state distribution, $1 \times N$
A	State transition probabilities, $N \times N$
B	Observation probability matrix, $N \times K$

We denote the elements in row i and column j of A as a_{ij} . The element a_{ij} of the A matrix is given by

$$a_{ij} = P(\text{state } q_j \text{ at } t+1 \mid \text{state } q_i \text{ at } t).$$

The (i, j) element of B is denoted in a slightly unusual form as $b_i(j)$. In a discrete HMM, row i of B represents the (discrete) probability distribution of the observation symbols when underlying Markov process is in (hidden) state i . Specifically, each element of $B = \{b_i(j)\}$ matrix is given by

$$b_i(j) = P(\text{observation } j \text{ at } t \mid \text{state } q_i \text{ at } t).$$

The HMM formulation can be used to solve the following three problems (Stamp, 2018).

1. Given an observation sequence O and a model λ of the form $\lambda = (\pi, A, B)$, calculate the probability of the observation sequence. That is, we can score an observation sequence against a given model.
2. Given a model $\lambda = (\pi, A, B)$ and an observation sequence O , find the “best” state sequence, where best is defined to be the sequence that maximizes the expected number of correct states. That is, we can uncover the hidden state sequence.
3. Given an observation sequence O , determine a model $\lambda = (A, B, \pi)$ that maximizes $P(O|\lambda)$. That is, we can train a model for a given observation sequence.

In this research, we are interested in problems 1 and 3. Specifically, we train models, then we test the resulting models by scoring observation sequences. The solution to problem 2 is of interest in various NLP applications, for example. For the sake of brevity, we omit the details of training and scoring with discrete HMMs; see (Stamp, 2018) or (Rabiner, 1989) for more information.

3.3 GMM-HMM

The structure of a GMM-HMM is similar to that of a discrete HMM. However, in a GMM-HMM, the B matrix is much different, since we are dealing with a mixture of (continuous) Gaussian distributions, rather than the discrete probability distributions a discrete HMM. In a GMM-HMM, the probability of an observation at a given state is determined by a probability density function that is defined by a GMM. Specifically, the probability density function of observation O_t when the model is in state i is given by

$$P_i(O_t) = \sum_{m=1}^M c_{im} g(O_t | \mu_{im}, \Sigma_{im}), \quad (1)$$

for $i \in \{1, 2, \dots, N\}$ and $t \in \{0, 1, \dots, T-1\}$, where

$$\sum_{m=1}^M c_{im} = 1 \text{ for } i \in \{1, 2, \dots, N\}.$$

Here, M is the number of Gaussian mixtures components, c_{im} is the mixture coefficient or the weight of m^{th} Gaussian mixture at state i , while μ_{im} and Σ_{im} are the mean vector and covariance matrix for the m^{th} Gaussian mixture at state i . We can rewrite g in equation (1) as

$$g(O_t | \mu_{im}, \Sigma_{im}) = \frac{1}{(2\pi)^{\frac{D}{2}} |\Sigma_{im}|^{\frac{1}{2}}} e^{-\frac{1}{2}(O_t - \mu_{im})' \Sigma_{im}^{-1} (O_t - \mu_{im})},$$

where D is the dimension of each observation. In a GMM-HMM, the A and π matrices are the same as in a discrete HMM.

The notation for a GMM-HMM is given in Table 2. This is inherently more complex than a discrete HMM, due to the presence of the M Gaussian distributions. Note that a GMM-HMM is defined by the 5-tuple

$$\lambda = (A, \pi, c, \mu, \Sigma).$$

Table 2: GMM-HMM notation

Notation	Explanation
T	Length of the observation sequence
O	Observation sequence, O_0, O_1, \dots, O_{T-1}
N	Number of states in the model
M	Number of Gaussian components
D	Dimension of each observation
π	Initial state distribution, $1 \times N$
A	State transition matrix, $N \times N$
c	Gaussian mixture weight at each state, $N \times M$
μ	Means of Gaussians at each state, $N \times M \times D$
Σ	Covariance of Gaussian mixtures, $N \times M \times D \times D$

Analogous to a discrete HMM, we can solve the same three problems with a GMM-HMM. However, the process used for training and scoring with a GMM-HMM differ significantly as compared to a discrete HMM.

3.4 GMM-HMM Training and Scoring

To use a GMM-HMM to classify malware samples, we need to train a model, then use the resulting model to score samples—see the discussion of problems 1 and 3 in Section 3.2, above. In this section, we discuss scoring and training in the context of a GMM-HMM in some detail. We begin with the simpler problem, which is scoring.

3.4.1 GMM-HMM Scoring

Given a GMM-HMM, which is defined by the 5-tuple of matrices $\lambda = (A, \pi, c, \mu, \Sigma)$, and a sequence of observations $O = \{O_0, O_1, \dots, O_{T-1}\}$, we want to determine $P(O|\lambda)$. The forward algorithm, which is also known as the α -pass, can be used to efficiently compute $P(O|\lambda)$.

Analogous to a discrete HMM as discussed in (Stamp, 2018), in the α -pass of a GMM-HMM, we define

$$\alpha_t(i) = P(O_0, O_1, \dots, O_t, x_t = q_i | \lambda),$$

that is, $\alpha_t(i)$ is the probability of the partial sequence of observation up to time t , ending in state q_i at time t . The desired probability is given by

$$P(O | \lambda) = \sum_{i=0}^{N-1} \alpha_{T-1}(i).$$

The $\alpha_t(i)$ can be computed recursively as

$$\alpha_t(i) = \left(\sum_{j=0}^{N-1} \alpha_{t-1}(j) a_{ji} \right) b_i(O_t). \quad (2)$$

At time $t = 0$, from the definition it is clear that we have $\alpha_0(i) = \pi_i b_i(O_0)$.

In a discrete HMM, $b_i(O_t)$ gives the probability of observing O_t at time t when the underlying Markov process is in state i . In a GMM-HMM, however, simply replacing $b_i(O_t)$ in (2) by the GMM pdf corresponds to a point value of a continuous distribution. To obtain the desired probability, as discussed in (Nguyen, 2016), we must integrate over of a small region around observation O_t , that is, we compute

$$b_i(O_t) = \int_{O_t - \varepsilon}^{O_t + \varepsilon} p_i(O_t | \theta_i) dO, \quad (3)$$

where θ_i consists of the parameters c_i , μ_i and Σ_i of the GMM, and ε is a (small) range parameter.

3.4.2 GMM-HMM Training

The forward algorithm or α -pass calculates the probability of observing the sequence from the beginning up to time t . There is an analogous backwards pass or β -pass that calculates the probability of the tail of the sequence, that is, the sequence from $t + 1$ to the end. In the β -pass, we define

$$\beta_t(i) = P(O_{t+1}, O_{t+2}, \dots, O_{T-1} | x_t = q_i, \lambda).$$

The $\beta_t(i)$ can be compute recursively via

$$\beta_t(i) = \sum_{j=0}^{N-1} a_{ij} b_j(O_t) \beta_{t+1}(j)$$

where we the initialization is $\beta_{T-1}(i) = 1$, which follows from the definition.

In a discrete HMM, to re-estimate the state transitions in the A matrix, we first define

$$\gamma_t(i, j) = P(x_t = q_i, x_{t+1} = q_j | O, \lambda)$$

which is the probability of being in state q_i at time t and transiting to state q_j at time $t + 1$. Using the α -pass and the β -pass, we can efficiently compute $\gamma_t(i, j)$; see (Stamp, 2018) for the details. The sum of these “di-gamma” values with respect to the transiting states gives the probability of the observation being in state q_i at time t , which we define as $\gamma_t(i)$. That is,

$$\gamma_t(i) = \sum_{j=1}^N \gamma_t(i, j).$$

Thus, we can re-estimate the elements of the A matrix in a discrete HMM as

$$a_{ij} = \frac{\sum_{t=0}^{T-2} \gamma_t(i, j)}{\sum_{t=0}^{T-2} \gamma_t(i)}$$

To train a GMM-HMM, we use an analogous strategy as that used for the discrete HMM. The GMM-HMM analog of the di-gamma form is

$$\gamma_t(j, k) = P(x_t = q_j | k, O, \lambda),$$

where $t = 0, 1, \dots, T-2$, and $j = 1, 2, \dots, N$, and we have $k = 1, 2, \dots, M$. Here, $\gamma_t(j, k)$ represents the probability of being state q_j at time t with respect to the k^{th} Gaussian mixture. According to (Rabiner, 1989), these $\gamma_t(j, k)$ are computed as

$$\gamma_t(j, k) = \frac{\alpha_t(j)\beta_t(j)}{\sum_{j=1}^N \alpha_t(j)\beta_t(j)} \cdot \frac{c_{jk}N(O_t | \mu_{jk}, \Sigma_{jk})}{\sum_{m=1}^M c_{jm}N(O_t | \mu_{jm}, \Sigma_{jm})}$$

where the $\alpha_t(j)$ and $\beta_t(j)$ are defined above, and c_{jk} is the weight of the k^{th} Gaussian mixture component.

The re-estimates for the weights c_{jk} of the Gaussian mixtures are given by

$$\hat{c}_{jk} = \frac{\sum_{t=0}^{T-1} \gamma_t(j, k)}{\sum_{t=0}^{T-1} \sum_{k=1}^M \gamma_t(j, k)}, \quad (4)$$

for $j = 1, 2, \dots, N$ and $k = 1, 2, \dots, M$; see (Juang, 1985) and (Rabiner, 1989) for additional details. The numerator in (4) can be interpreted as the expected number of transitions from state q_j as determined by the k^{th} Gaussian mixture while the denominator can be viewed as the expected transitions from state q_j given by the M Gaussian mixtures. Accordingly, the re-estimation for μ_{jk} and Σ_{jk} are of the form

$$\hat{\mu}_{jk} = \frac{\sum_{t=0}^{T-1} \gamma_t(j, k) O_t}{\sum_{t=0}^{T-1} \gamma_t(j, k)}$$

and

$$\hat{\Sigma}_{jk} = \frac{\sum_{t=0}^{T-1} \gamma_t(j, k) (O_t - \mu_{jk})(O_t - \mu_{jk})'}{\sum_{t=0}^{T-1} \gamma_t(j, k)},$$

for $i = 1, 2, \dots, N$ and $k = 1, 2, \dots, M$.

3.5 GMM-HMM Example

As an example to illustrate a GMM-HMM, we train a model on English text, which is a classic example for discrete HMMs (Cave and Neuwirth, 1980). With $N = 2$ hidden states and $M = 27$ observation symbols (corresponding to the 26 letters and word-space), a discrete HMM trained on English text will have one hidden state corresponding to consonants, while the other hidden state corresponds to vowels. That the model can make this key distinction is a good example of learning, since a priori no information is provided regarding the differences between the observations. We consider this same experiment using a GMM-HMM to see how this model compares to a discrete HMM.

The English training data is from the ‘‘Brown corpus’’ (Brown Corpus of standard American English, 1961), and we convert all letters to lowercase and remove punctuation, numbers, and other special symbols, leaving only 26 letters and word-spaces. For our GMM-HMM training, we set $N = 2$, $M = 6$ (i.e., we have a mixture model consisting of 6 Gaussians) and $T = 50000$. The A matrix is $N \times N$, π is $1 \times N$, both of which are row stochastic, and initialized to approximately uniform. The parameter c represents the weights of the mixture components and is initialized with row stochastic values, also approximately uniform. We use the global mean value (i.e., the mean of all observations) and global variance to initialize μ and Σ . Note that each Gaussian is initialized with the same mean and variance.

We train 100 of these GMM-HMM models, each with different random initializations. As the observations are discrete symbols, the probability of each observation in state i at time t is estimated by the probability density function. The best of the trained models clearly shows that the GMM-HMM technique is able to successfully group the vowels into one state. This can be seen from Figure 1. Note that in Figure 1, word-space is represented by the symbol ‘‘_’’.

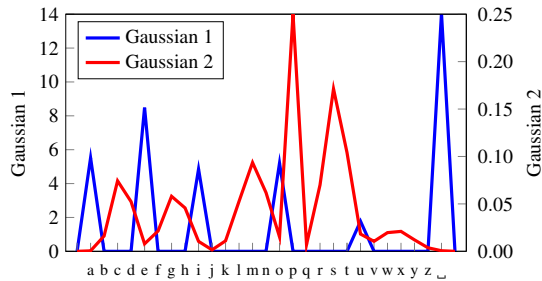


Figure 1: English letter distributions in each state

Table 3: Mean of each Gaussian mixture in each state

State	Gaussian					
	1	2	3	4	5	6
0	26.00	14.00	8.00	4.00	20.00	0.00
1	22.60	6.31	15.00	12.08	2.31	18.14

Figure 1 clearly shows that all vowels (and word space) belong to the first state. Table 3 lists the mean value for each Gaussian mixture in the trained model. The mean value of each Gaussian mixture component corresponds to the encoded value of each observation symbol.

In this example, since we know the number of vowels beforehand, we have set the number of Gaussian mixture components to 6 (i.e., 5 vowels and word-space). In practice, we generally do not know the true number of hidden states, in which case we would need to experiment with different numbers of Gaussians. In general, machine learning and deep learning requires a significant degree of experimentation, so it is not surprising that we might need to fine tune our models.

4 Malware Experiments

In this section, we first introduce the dataset used in our experiments, followed by two distinct sets of experiments. In our first set of experiments, we compare the performance of discrete HMMs and GMM-HMMs using opcode sequences as our features. In our second set of experiments, we consider entropy sequences, which serve to illustrate the strength of the GMM-HMM technique.

4.1 Dataset

In all of our experiments, we consider three malware families, namely, Winwebsec, Zbot, and Zeroaccess.

Winwebsec is a type of Trojan horse in the Windows operating system. It attempts to install malicious programs by displaying fake links to bait users (Winwebsec, 2017).

Zbot is another type of Trojan that tries to steal user information by attaching executable files to spam email messages (Zbot, 2017).

Zeroaccess also tries steal information, and it can also cause other malicious actions, such as downloading malware or opening a backdoor (Neville and Gibb, 2013).

Table 4 lists the number of samples of each malware family in our dataset. These families are part of the Malicia dataset (Nappa et al., 2015) and have been used in numerous previous malware studies.

The samples of each malware family are split into 80% for training and 20% for testing. We train models on one malware family, and test the resulting model separately against the other two families. Note that each of these experiments is a binary classification problem.

We use the area under the ROC curve (AUC) as our measure of success. The AUC can be interpreted as the probability that a randomly selected positive sample scores higher than a randomly

Table 4: Number of samples in each malware family

Family	Samples
Winwebsec	4360
Zeroaccess	2136
Zbot	1305
Total	7801

Table 5: Percentage of top 30 opcodes

Family	Top 30 opcodes
Winwebsec	96.9%
Zeroaccess	95.8%
Zbot	93.4%

selected negative sample (Bradley, 1997). We perform 5-fold cross validation, and the average AUC from the 5 folds is the numerical result that we use for comparison.

4.2 Opcode Features

For our first set of malware experiments, we compare a discrete HMM and GMM-HMM using mnemonic opcode sequences as features. To encode the input, we disassemble each executable, then extract the opcode sequence. We retain the most frequent 30 opcodes with all remaining opcodes lumped together into a single “other” category, giving us a total of 31 distinct observations. The percentage of opcodes that are among the top 30 most frequent are listed in Table 5.

For training, we limit the length of the observation sequence to $T = 100000$, and for the discrete HMM, we let $N = 2$. For the GMM-HMM, we experiment with the number of Gaussian mixtures ranging from $M = 2$ to $M = 5$.

As mentioned above, we train a model with one malware family and test with the other two malware families individually (i.e., in binary classification mode). To test each model’s performance, we use one hundred samples from both families in the binary classification.

We initialize π and A to be approximately uniform, as well as making them row stochastic. For each discrete HMM, the B matrix is initialize similarly, while for each GMM-HMM, the mean values and the covariance are initialized with the global mean value and the global covariance of all training samples.

Figure 2 gives the average AUC (over the 5 folds) for models trained with discrete HMMs and the GMM-HMMs with different values for m , the number of Gaussians in the mixture. For most of the models, the GMM-HMM is able to obtain comparable results to the discrete HMM, and it does slightly outperform a discrete HMM in some cases. but the improvement is slight.

The results in Figure 2 indicate that for opcodes sequences, GMM-HMMs perform comparably to discrete HMMs. However, GMM-HMMs are more complex and more challenging to train, and the additional complexity does not appear to be warranted in this case. But, this is not surprising, as opcode sequences are inherently discrete features. To obtain a more useful comparison, we next consider GMM-HMMs trained on continuous features.

4.3 Entropy Features

GMM-HMMs are designed for continuous data, as opposed to discrete features, such as opcodes. Thus to take full advantage of the GMM-HMM technique, we consider continuous entropy based features.

We use a similar feature-extraction method as in (Baysa et al., 2013). Specifically, we consider the raw bytes of an executable file, and we define a window size over which we compute the entropy.

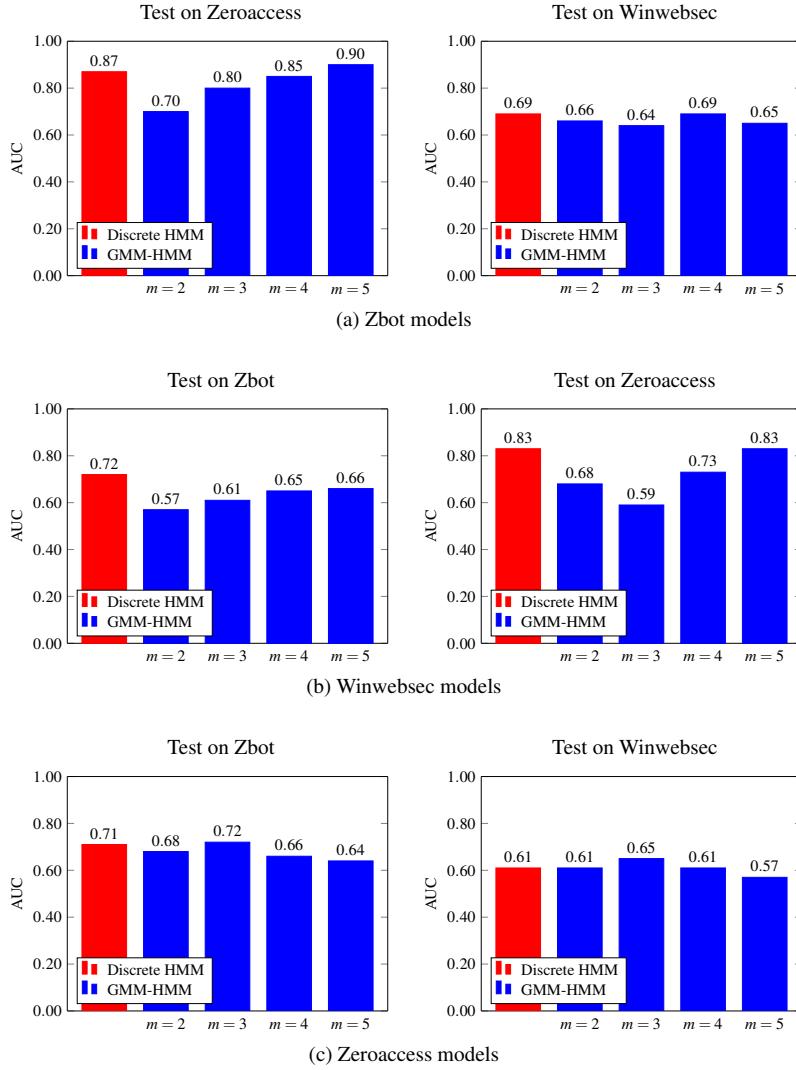


Figure 2: Average AUC

Then we slide the window by a fixed amount and repeat the entropy calculation. Both the window size and the slide amount are parameters that need to be tuned to obtain optimal performance. In general, the slide will be smaller than the window size to ensure no information is lost.

Entropy is computed using Shannon’s well known formula (Togneri and DeSilva, 2003)

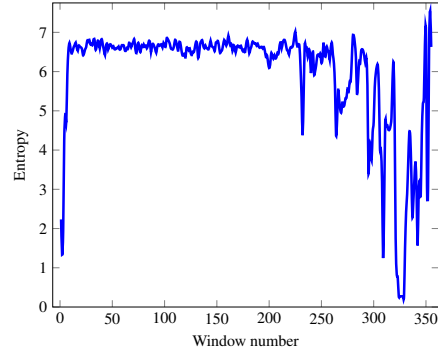
$$E = - \sum_{x \in W_i} p(x) \log_2 p(x),$$

where W_i is the i^{th} window, and $p(x)$ is the frequency of the occurrence of byte x within window W_i .

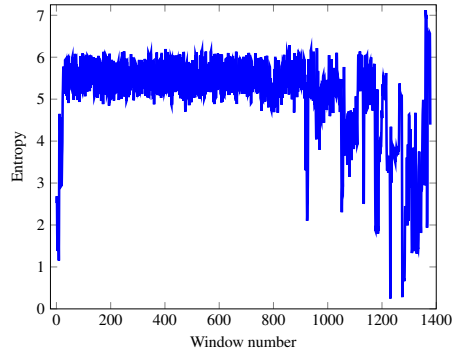
The entropy tends to be smoothed out with larger window sizes. We want to select a window size sufficiently large so that we reduce noise, but not so large as to lose useful information. Examples of entropy plots for different parameters are given in Figure 3.

Based on the results in (Baysa et al., 2013), we use half of the window size as the slide amount. To select the best values for the parameters, we conduct experiments with the window and slide combinations listed in Table 6. Also, as part of the parameter tuning process, we selected ϵ in (3) to be 0.000001 for both Zbot and Zeroaccess, while we find 0.1 is optimal for Winwebsec.

For models trained on Zbot, the results of our experiments with the different window and slide



(a) Window size = 512



(b) Window size = 128

Figure 3: Entropy plots

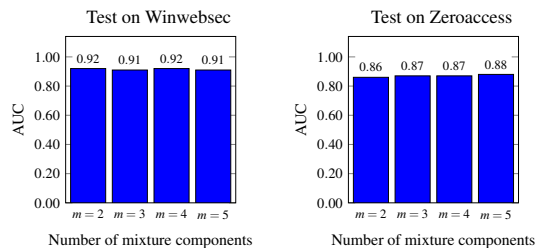
Table 6: Window size and slide amount

Window size	512	256	128
Slide	256	128	64

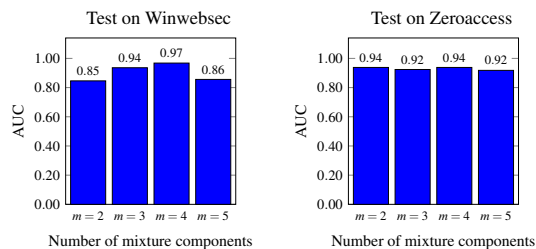
size pairings in Table 6 are given in Figure 4. The corresponding bar graphs for models trained on Winwebsec and Zeroaccess are given in Figures 5 and 6, respectively, which can be found in the Appendix. Note that we have experimented with the number of Gaussians in our mixture ranging from $m = 2$ to $m = 5$. We see that a window size of size 512 performs the worst, while window sizes of size 256 and 128 give improved results, with size 128 being slightly better than 256. The optimal number of Gaussians depends on the families we are classifying. The results of analogous experiments training models on Winwebsec and Zeroaccess are given in Figures 5 and 6, respectively.

In Table 7, we provide a direct comparison of discrete HMMs trained on opcodes to GMM-HMM trained on opcodes and the best GMM-HMM models trained on entropy sequences. In every case, the entropy-trained GMM-HMM outperforms the corresponding opcode based models. It is also worth noting that computing an entropy sequence is more efficient than extracting mnemonic opcodes. While it is costlier to train a GMM-HMM, the scoring cost is similar to a discrete HMM. Since training is one-time work, efficiency considerations also favor entropy-based GMM-HMMs.

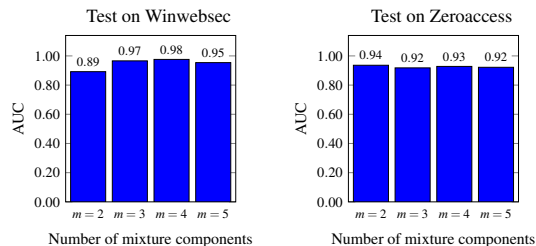
From Table 7 we see that GMM-HMMs trained on entropy perform dramatically better than discrete HMMs, except in the two cases where models where Zbot and Zeroaccess are involved. To gain further insight into these anomalous case, we use the Kullback–Leibler (KL) divergence (Joyce, 2011) to compare the probability distributions defined by of our trained GMM-HMM models. The



(a) Window size = 512



(b) Window size = 256



(c) Window size = 128

Figure 4: Entropy vs window size for Zbot models

Table 7: Comparison of discrete HMM and GMM-HMM

Train	Test	Opcode HMM	Opcode GMM-HMM	Entropy GMM-HMM
Zbot	Zeroaccess	0.87	0.90	0.94
Zbot	Winwebsec	0.69	0.69	0.98
Zeroaccess	Zbot	0.71	0.72	0.77
Zeroaccess	Winwebsec	0.61	0.65	0.99
Winwebsec	Zbot	0.72	0.66	1.00
Winwebsec	Zeroaccess	0.83	0.83	1.00

KL divergence between two probability distributions is given by

$$\text{KL}(p \parallel q) = \int_{-\infty}^{\infty} p(x) \log \frac{p(x)}{q(x)}, \quad (5)$$

where p and q are probability density functions. Note that the KL divergence in (5) is not symmetric, and hence not a true distance measure. We compute a symmetric version of the divergence for models \mathcal{M}_1 and \mathcal{M}_2 as

$$\text{KL}(\mathcal{M}_1, \mathcal{M}_2) = \frac{\text{KL}(\mathcal{M}_1 \parallel \mathcal{M}_2) + \text{KL}(\mathcal{M}_2 \parallel \mathcal{M}_1)}{2}. \quad (6)$$

Using equation (6) we obtain the (symmetric) divergence results in Table 8. We see that the Zbot and Zeroaccess models are much closer in terms of KL divergence, as compared to the other two pairs. Thus we would expect GMM-HMM models to have more difficulty distinguishing these two families from each other, as compared to the models generated for the other pairs of families.

Table 8: The KL divergence of different models

Models	KL divergence
Zbot, Zeroaccess	611.58
Zbot, Winwebsec	1594.05
Zeroaccess, Winwebsec	1524.39

Curiously, the models trained on Zbot and tested on Zeroaccess perform well.¹ Hence, a relatively small KL divergence does not rule out the possibility that models can be useful, but intuitively, a large divergence would seem to be an indicator of potentially challenging cases. This issue requires further study.

5 Conclusion and Future Work

In this paper, we have explored the usage of GMM-HMMs for malware classification. We compared GMM-HMMs to discrete HMMs using opcode sequences, and we further experimented with entropy sequences as features for GMM-HMMs. With the opcode sequence features, we were able to obtain results with GMM-HMMs that are comparable to those obtained using discrete HMMs. However, we expect GMM-HMMs to perform best on features that are naturally continuous, so we also experimented with byte-based entropy sequences. In this latter set of experiments, the GMM-HMM technique yielded stronger results than the discrete HMM in all cases—and in four of the six cases, the improvement was large. We also directly compared the GMMs of our trained models using KL divergence, which seems to provide insight into the most challenging cases.

For future work, more extensive experiments over larger numbers of families with larger numbers of samples per family would be valuable. True multiclass experiments based on GMM-HMM scores would also be of interest. Further analysis of the KL divergence of GMM-HMMs might provide useful insights into these models.

References

- Alfakih, M., Keche, M., Benoudnine, H., and Meche, A. (2020). Improved Gaussian mixture modeling for accurate Wi-Fi based indoor localization systems. *Physical Communication*, 43.
- Bansal, P., Kant, A., Kumar, S., Sharda, A., and Gupta, S. (2008). Improved hybrid model of hmm/gmm for speech recognition. In *International Conference on Intelligent Information and Engineering Systems*, INFOS 2008.
- Baysa, D., Low, R., and Stamp, M. (2013). Structural entropy and metamorphic malware. *Journal of Computer Virology and Hacking Techniques*, 9(4):179–192.
- Ben Abdel Ouahab, I., Bouhorma, M., Boudhir, A. A., and El Aachak, L. (2020). Classification of grayscale malware images using the k -nearest neighbor algorithm. In Ben Ahmed, M., Boudhir, A. A., Santos, D., El Aroussi, M., and Karas, Í. R., editors, *Innovations in Smart Cities Applications*, pages 1038–1050. Springer, 3 edition.
- Bradley, A. P. (1997). The use of the area under the ROC curve in the evaluation of machine learning algorithms. *Pattern Recognition*, 30(7):1145–1159.
- Brown Corpus of standard American English (1961). The Brown corpus of standard American English. <http://www.cs.toronto.edu/~gpenn/csc401/alres.html>.
- Cave, R. L. and Neuwirth, L. P. (1980). Hidden Markov models for English. In Ferguson, J. D., editor, *Hidden Markov Models for Speech*. IDA-CCR.
- Chen, Y. and Wu, W. (2019). Separation of geochemical anomalies from the sample data of unknown distribution population using gaussian mixture model. *Computers & Geosciences*, 125:9–18.

¹It is worth noting that the opcode based models also performed well in this case.

- Dang, S., Chaudhury, S., Lall, B., and Roy, P. K. (2017). Learning effective connectivity from fMRI using autoregressive hidden Markov model with missing data. *Journal of Neuroscience Methods*, 278:87–100.
- Fraley, C. and Raftery, A. E. (2002). Model-based clustering, discriminant analysis, and density estimation. *Journal of the American Statistical Association*, 97(458):611–631.
- Gallop, J. (2006). Facies probability from mixture distributions with non-stationary impedance errors. In *SEG Technical Program Expanded Abstracts 2006*, pages 1801–1805. Society of Exploration Geophysicists.
- Gao, Z., Sun, Z., and Liang, S. (2020). Probability density function for wave elevation based on Gaussian mixture models. *Ocean Engineering*, 213.
- Guoning Hu and DeLiang Wang (2004). Monaural speech segregation based on pitch tracking and amplitude modulation. *IEEE Transactions on Neural Networks*, 15(5):1135–1150.
- Interrante-Grant, A. M. and Kaeli, D. (2018). Gaussian mixture models for dynamic malware clustering. https://coe.northeastern.edu/wp-content/uploads/pdfs/coe/research/embark/4-interrante-grant.alex_final.pdf.
- Joyce, J. M. (2011). Kullback-Leibler divergence. In Lovric, M., editor, *International Encyclopedia of Statistical Science*, pages 720–722. Springer.
- Juang, B. (1985). Maximum-likelihood estimation for mixture multivariate stochastic observations of Markov chains. *AT&T Technical Journal*, 64(6):1235–1249.
- Kalash, M., Rochan, M., Mohammed, N., Bruce, N. D. B., Wang, Y., and Iqbal, F. (2018). Malware classification with deep convolutional neural networks. In *2018 9th IFIP International Conference on New Technologies, Mobility and Security*, NTMS, pages 1–5.
- Kruczkowski, M. and Szykiewicz, E. N. (2014). Support vector machine for malware analysis and classification. In *2014 IEEE/WIC/ACM International Joint Conferences on Web Intelligence and Intelligent Agent Technologies*, WI-IAT '14, pages 415–420.
- Laraba, S. and Tilmann, J. (2016). Dance performance evaluation using hidden Markov models. *Computer Animation and Virtual Worlds*, 27(3-4):321–329.
- McLachlan, G. and Peel, D. (2004). *Finite Mixture Models*. Wiley.
- Milosevic, N. (2013). History of malware. <https://arxiv.org/abs/1302.5392>.
- Nappa, A., Rafique, M. Z., and Caballero, J. (2015). The MALICIA dataset: Identification and analysis of drive-by download operations. *International Journal of Information Security*, 14(1):15–33.
- Neville, A. and Gibb, R. (2013). ZeroAccess Indepth. <https://docs.broadcom.com/doc/zeroaccess-indepth-13-en>.
- Nguyen, L. (2016). Continuous observation hidden Markov model. *Revista Kasma*, 44(6):65–149.
- Qiao, J., Cai, X., Xiao, Q., Chen, Z., Kulkarni, P., Ferris, C., Kamarthi, S., and Sridhar, S. (2019). Data on MRI brain lesion segmentation using k -means and Gaussian mixture model-expectation maximization. *Data in Brief*, 27.
- Rabiner, L. R. (1989). A tutorial on hidden Markov models and selected applications in speech recognition. *Proceedings of the IEEE*, 77(2):257–286.
- Raitoharju, M., García-Fernández, A., Hostettler, R., Piché, R., and Särkkä, S. (2020). Gaussian mixture models for signal mapping and positioning. *Signal Processing*, 168:107330.
- Reynolds, D. (2015). Gaussian mixture models. In Li, S. Z. and Jain, A. K., editors, *Encyclopedia of Biometrics*, pages 827–832. Springer.
- Stamp, M. (2018). A revealing introduction to hidden Markov models. <https://www.cs.sjsu.edu/~stamp/RUA/HMM.pdf>.
- Stanculescu, I., Williams, C. K. I., and Freer, Y. (2014). Autoregressive hidden Markov models for the early detection of neonatal sepsis. *IEEE Journal of Biomedical and Health Informatics*, 18(5):1560–1570.
- Togneri, R. and DeSilva, C. J. S. (2003). *Fundamentals of Information Theory and Coding Design*. CRC Press.

Truong, A. and Zaharia, T. (2017). Laban movement analysis and hidden Markov models for dynamic 3D gesture recognition. *EURASIP Journal on Image and Video Processing*, 2017.

Winwebsec (2017). Win32/winwebsec threat description - Microsoft security intelligence. <https://www.microsoft.com/en-us/wdsi/threats/malware-encyclopedia-description?Name=Win32/Winwebsec>.

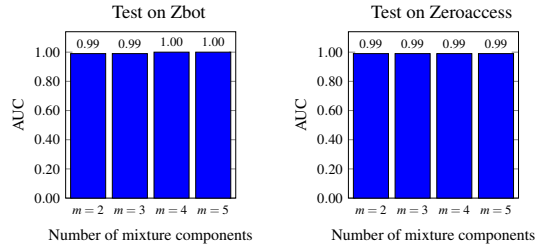
Yao, Z., Ge, J., Wu, Y., Lin, X., He, R., and Ma, Y. (2020). Encrypted traffic classification based on Gaussian mixture models and hidden Markov models. *Journal of Network and Computer Applications*, 166.

Zbot (2017). Pws:win32/zbot threat description - Microsoft security intelligence. <https://www.microsoft.com/en-us/wdsi/threats/malware-encyclopedia-description?Name=PWS%3AWin32%2FZbot>.

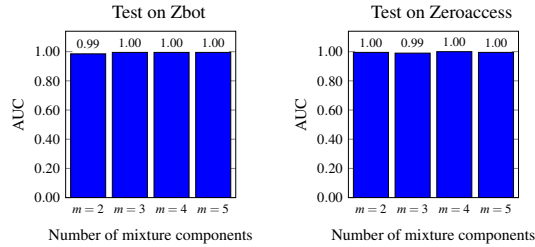
Zhang, F., Han, S., Gao, H., and Wang, T. (2020). A Gaussian mixture based hidden Markov model for motion recognition with 3D vision device. *Computers & Electrical Engineering*, 83.

APPENDIX

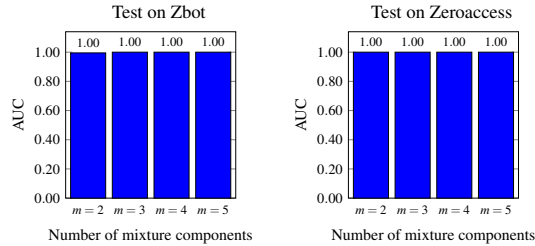
Here, we bar graphs analogous to those in Figure 4 for models trained on Winwebsec and Zeroaccess.



(a) Window size = 512

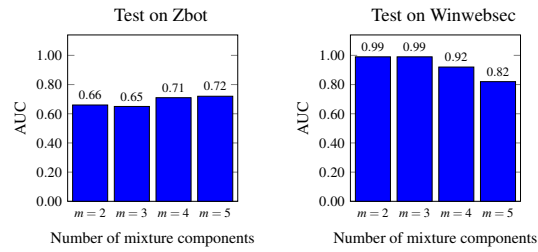


(b) Window size = 256

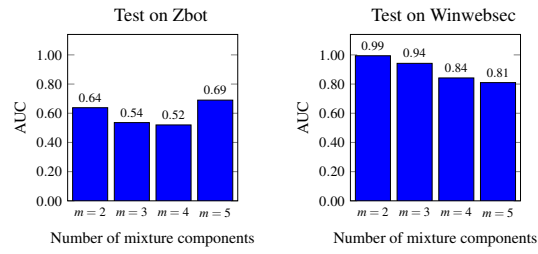


(c) Window size = 128

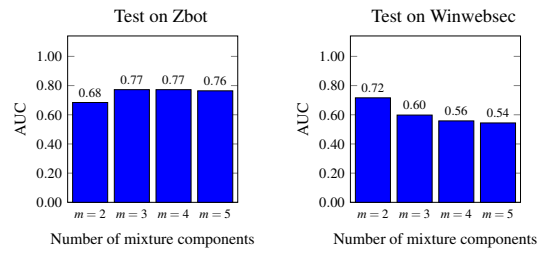
Figure 5: Entropy vs window size for Winwebsec models



(a) Window size = 512



(b) Window size = 256



(c) Window size = 128

Figure 6: Entropy vs window size for Zeroaccess models